Policy Research Journal
ISSN (E): 3006-7030 ISSN (P) : 3006-7022 Volume 4, Issue 2, 2026

SOIL EROSION SUSCEPTIBILITY MAPPING USING REMOTE SENSING AND GIS OF DISTRICT KOHAT, KHYBER PAKHTUNKHWA PAKISTAN

Mehran Ahmad[1], Maryam Khalid[2], Umair Aftab Choudary[3], Saqib Ullah[4], Muhammad Ishfaq[*5], Zeeshan Khattak[6], Sobia Rani[7]

[1]*Meteorolgy (Rs and GIS), COMSATS University Islamabad*
[2] *Lecturer, Institute of Geography, University of the Punjab, Lahore Pakistan MS*
[3] *MS Scholar, Bahria University, Islamabad*
[4] *MS Scholar, NCEG Peshawar*
[*5] *Meteorology (Rs and GIS), COMSATS University Islamabad*
[6]*Project Geologist at Geological Survey of Pakistan, Peshawar*
[7]*GIS Analyst at Gravity Solution, Islamabad*

[1]mehrankhanmnd@gmail.com, [2]maryamkhalid.geog@pu.edu.pk, [3]umair7906@gmail.com, [4]saqib.ktk337@gmail.com, [*5]ishfaqgeo.gis@gmail.com, [6]zeshankhattak2611@gmail.com, [7]sobiarani853@gmail.com

DOI: https://doi.org/10.5281/zenodo.18638187

Keywords

Article History
Received: 15 December 2025
Accepted: 30 January 2026
Published: 14 February 2026

Corresponding Author: *
Muhammad Ishfaq

Abstract

Water and air are the major sources of soil erosion occurs which usually cause soils to progressively disappear from its surface. To understand this phenomenon and to efficiently develop a management plan in District Kohat, Pakistan, this research was aimed to map soil erosion susceptibility across the district and to identify the associated factors using geospatial techniques. Elevation, Slope aspect, curvature, land use, land cover, lithology, soil texture, rainfall, drainage, and roadways were among the characteristics that were the focus of the current study. ALOS, top sheets, land use land cover, the Geological Survey of Pakistan's soil structure map, and Google Earth pictures were some of the sources from which data was gathered for this study. All the layer was reclassified high weightage were given to the high influencing factor and low weightage were given to the low influencing factor. All the reclassified layers were then incorporated in the weighted overlay analysis. According to the study's findings, 4% of soil erosion happened in the District Kohat along center part of the drainage, but some areas saw remapping. This system will generate comprehensive vulnerability maps by utilizing machine learning algorithms, remote sensing techniques, and sophisticated geospatial data. Sustainable land management techniques, conservation programs, and land use planning will all be based on these maps. The produced maps enable erosion prevention and control strategies to be prioritized by giving decision makers access to relevant information. In the end, this project's vulnerability map will be a useful tool for sustainable development, land management, and conservation initiatives.

INTRODUCTION

1.1 Background

Soil erosion is the process by which soil is gradually removed from its surface due to external factors such as water or air (Maity *et al.*, 2019).

Water, particularly through the force of raindrops and flowing water, is the primary cause of soil disintegration, involving phases like soil particle detachment, transportation, and sediment deposition (Jebur *et al.*, 2014). This natural phenomenon significantly impacts ecosystems and alters soil properties, including its organic, physical, and chemical composition it's widely recognized as a critical threat to soil sustainability, responsible for approximately 80% of global land degradation on agricultural land (Puente *et al.*, 2019). The effects are severe, ranging from decreased agricultural productivity to compromised water quality, increased landslide risks on steep terrain, and sediment deposition in reservoirs leading to heightened flood hazards and reduced hydro energy generation (Alexander *et al.*, 2012).Addressing these challenges necessitates sustainable management practices that involve measuring soil erosion, spatially mapping its distribution, and identifying vulnerable areas using susceptibility analysis (Koirala *et al.*, 2019). Interrelated aspects such as precipitation, topography, soil characteristics, and LULC management contribute to land degradation (Yusof *et al.*, 2014). Anthropogenic activities like urbanization, unsustainable farming methods, mining, and deforestation exacerbate soil degradation, placing additional strain on natural ecosystems (Smith *et al.*, 2016). Processes like gully and rill erosion lead to sediment laden water, causing river channel erosion and further exacerbating soil loss along riverbanks, contributing to excessive erosion and sedimentation in floodplain areas (Sahaar *et al.*, 2013). Overall, soil erosion poses a significant global challenge, impacting agricultural productivity and ecosystem health by depleting topsoil nutrients and minerals. It's estimated that millions of acres of agricultural land are lost to erosion annually, resulting in decreased agricultural output and economic vulnerabilities. Globally, rates of soil loss exceed soil development rates by a factor of 10–40, posing threats to both food security and environmental integrity (Across Asia, the annual average soil loss rate is 29.95 t/ha/y, highlighting the urgent need for soil conservation efforts (Price *et al.*, 2014). Asian rivers contribute approximately eighty percent of the sediment discharged into the world's oceans (Naqvi *et al.*, 2013). Exacerbating soil degradation and necessitating effective management strategies. Erosion susceptibility analysis evaluates the likelihood of erosion events based on past occurrences and causal factors (Ettazarini *et al.*, 2017).

Water-induced soil erosion and land degradation are major environmental issues in Pakistan. According to Ashraf *et al.* (2017), 11.2 million hectares (M.ha) or 70% of Pakistan's land is impacted by water erosion, while the remaining 16 million M.ha (approximately 20%) of land are affected by soil erosion. Topography, vegetation type, soil qualities, and land use are some of the elements that greatly impact the phenomenon of soil erosion. Nitrogen-rich topsoil is eroded by flash floods and leaf erosion, which significantly slows down plant growth. Additionally, more permeable subsurface layers cause more runoff, which restricts the amount of water available for plant growth. Additionally, because of eroded particles and sediment loading, erosion also has a number of off-site effects, such as poor water quality. In Pakistan's dry regions, agricultural disasters can arise from nutrient loss and soil deterioration brought on by water erosion. The scientific community continues to face challenges from the increased interest in protecting the socio-agricultural ecosystem and maintaining water resources in arid places in order to prevent global food shortages. Pakistan's major source of erosion is water, and the province of Kohat Pakhtunkhwa is the most severely affected (Samina *et al.*, 2010). This study approach to mapping soil erosion susceptibility is essential for effective mitigation and management. The objective of this project is to develop a robust and precise soil erosion susceptibility mapping system capable of identifying and forecasting erosion-prone areas within a designated geographical area. This system will leverage advanced geospatial data, remote sensing techniques, and machine learning algorithms to generate detailed susceptibility maps. These maps will inform land-use planning,

conservation initiatives, and sustainable land management practices. By providing decision-makers with actionable insights, the resulting maps will enable the prioritization of erosion prevention and control measures. Ultimately, the susceptibility map produced by this project will serve as a valuable tool for land management, conservation efforts, and sustainable development. It will empower stakeholders to make informed decisions aimed at mitigating soil erosion and fostering sustainable land use practices.

1.2 Statement of the Problem

Soil erosion poses a significant environmental challenge, leading to land degradation and a decline in soil productivity (Liu *et al.*, 2020). This erosion-induced soil degradation is a critical ecological issue with far-reaching impacts on the environment, water quality, crop yields, and land resilience. Reduced fertility rates, damage to topsoil, and increased sedimentation in water basins are all consequences of soil erosion, disrupting the natural balance of soil composition and structure. The study area is particularly susceptible to soil erosion, mainly due to the prevalence of lithological formations and soil units prone to erosion. The instability of weathering rocks stems from a combination of external and internal factors. Key external influences include climatic variables and human activities, while internal factors involve geological composition, soil properties, and regional topography. Climatic variables encompass temperature and precipitation patterns, while human-induced factors encompass land use and land cover changes, road construction, dam building, and mining activities. Geological factors relate to the lithological makeup and presence of faults, while soil characteristics involve textural mapping. Topographic factors include elevation, slope, aspect, curvature, and lineament features. The current study area has been extensively studied by numerous researchers focusing on mineral exploration, hydrocarbon development, and groundwater exploration, utilizing a variety of techniques ranging from basic to advance. However, there remains a notable gap in research concerning soil erosion and its underlying factors within the Kohat region. Therefore, this present research aims to address this gap by investigating soil erosion in the Kohat region and examining its associated parameters. The study will employ GIS based Frequency Ratio Modeling (FRM) to map soil erosion, providing a comprehensive understanding of the phenomenon in the area. By filling this research gap, this study will serve as a foundational platform for future research endeavors pertaining to soil erosion in the region.

1.3.1 Study Area

The present study focuses on the Kohat region of Kohat Pakhtunkhwa, Pakistan as shown in Figure 1. The study area exhibits a limited steppe climate, characterized by minimal annual rainfall. Winters are brief, cold, and generally dry, while summers are long, wet, and sunny, with clear skies prevailing throughout the year. Extreme temperatures below -0.5°C and above 43.33°C are exceedingly rare, with typical temperatures ranging from 2.2°C to 39.45°C (Azra *et al.*, 2019). The Kohat plateau primarily consists of Miocene-Pliocene-aged clastic sedimentary rocks and Eocene-aged limestone, shale, evaporates, and subordinate clays (Hussain *et al.*, 2021). The plateau's geological age is characterized by Paleocene to Pliocene sedimentary strata, initially deposited on the northern Indian plate edge.

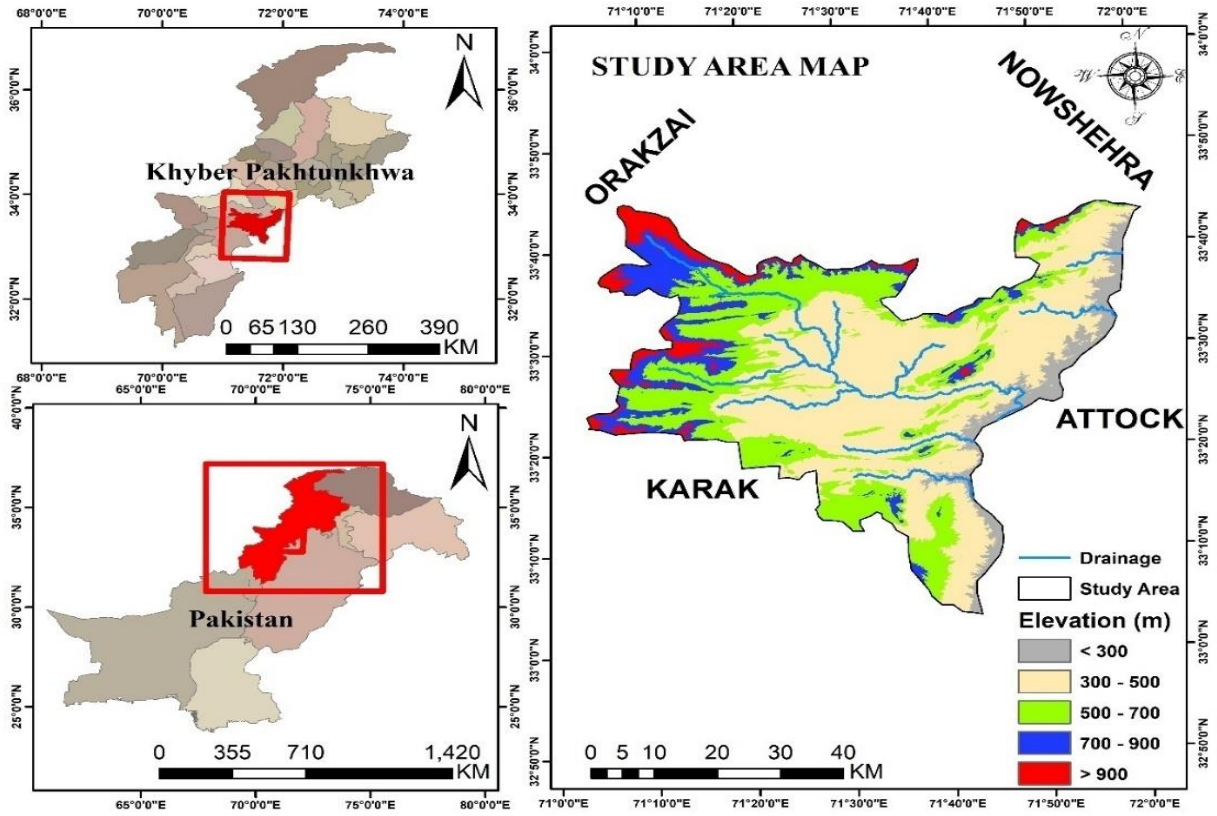

Figure 1.2 Study area map of District Kohat

1.3 Objectives of the study

The objectives of the present research are mentioned below;

- To identify the soil erosion hotspot areas in the District Kohat using RS/GIS techniques.
- To find out the causative factors of soil erosion in the study area.
- To generate a comprehensive final erosion susceptibility map to design and develop a mitigation strategy.

Literature Review

Researchers have developed Soil Erosion Susceptibility Mapping (SESM) using diverse methodologies and models (Igwe et al., 2020). Early soil mapping depended on field-based analyses, which are costly, labor-intensive, and often limited by inadequate sampling, thereby affecting spatial accuracy (Prasannakumar et al., 2011). Advances in mathematical and geospatial techniques now enable identification of erosion-prone areas through multiple models. Previous studies have proposed empirical equations for estimating runoff intensity and soil loss, generally involving data collection, model development, and evaluation stages (Kashiwar et al., 2022; Gong et al., 2022). Consideration of scale, erosion characteristics, and sectoral needs is essential (Senanayake et al., 2020). Prior to SESM development, qualitative approaches such as Weighted Overlay Analysis (WOA) and the Analytical Hierarchy Process (AHP) were widely applied to identify high-risk zones (Saha et al., 2019). WOA integrates factors like rainfall, terrain, and soil erodibility (Jabbar et al., 2019), while AHP—introduced by Saaty (1980)—is a structured multi-criteria decision-making method (Aslam et al., 2021). It verifies weight consistency through the consistency ratio (CR), where values

<0.1 indicate acceptable weighting. Other commonly used models include USLE, RUSLE, and MUSLE (Ganasri and Ramesh, 2016). RUSLE incorporates rainfall, topography, soil properties, and land use/cover, but is limited to sheet and rill erosion, excluding gully erosion (Thapa, 2020). Despite algorithmic uncertainties, their GIS compatibility ensures continued application (Tang et al., 2015). With GIS advancements, quantitative approaches using erosion inventory data as dependent variables and thematic layers as predictors have gained importance (Senanayake et al., 2020). Among bivariate models, the Frequency Ratio technique is extensively used to analyze erosion susceptibility and land-use relationships (Meena et al., 2023). Over the past decade, satellite remote sensing has become increasingly significant for erosion mapping due to improved data availability and resolution. Multispectral imagery, particularly Landsat, remains widely used despite limited high-spectral datasets (Sepuru and Dube, 2018). District-level Soil Erosion Risk (SER) mapping in Telangana identified priority conservation zones, revealing ~69% low-risk area, while districts such as Adilabad, Warangal, Khammam, and Karimnagar showed highest vulnerability (Biswas et al., 2015). Similarly, GIS-RUSLE applications in the Brazilian Amazon generated erosion risk maps using soil (K), topographic (LS), and canopy (C) factors derived from DEM and Landsat data, confirming lower erosion risk in forests compared to grazing lands (Lu et al., 2004). In India's Khajuri watershed, RUSLE-based GIS modeling estimated annual soil loss using R, K, LS, C, and P factors (Agarwal et al., 2016). Mountainous regions of Asia also face severe land degradation; RS-GIS integrated USLE modeling in northern Thailand mapped high vulnerability in shifting cultivation zones (Krishna, 2009). The Weight of Evidence (WOE) method has emerged as a statistical approach for spatial erosion prediction by integrating geomorphological, hydrological, climatic, and lithological factors (Hembram et al., 2019; Sharma et al., 2019). Evidential belief functions as a spatial probabilistic model of erosion processes (Chakraborty et al., 2020). Recently, qualitative and statistical methods have increasingly been complemented or replaced by machine learning techniques, which utilize historical datasets to predict erosion susceptibility (Arabameri et al., 2022; Chen et al., 2017; T Vu Dinh et al., 2021; Gayen et al., 2020; Rahmati et al., 2017).

Datasets and Methodology

The methodology of this study involves several key steps and is presented in a flowchart diagram as depicted in Figure 3.1. To achieve the objectives outlined in the study, the specific datasets were utilized. This dataset was comprised both ground remote sensing (RS) data, which is employed to generate a soil erosion map. The ground data is sourced from diverse national public and private research sectors. Satellite data is also playing a crucial role in this study, providing various parameters. Specifically, Sentinel-2, Advanced Land Observing Satellite (ALOS) DEM, and CHIRPS data were utilized. The ALOS DEM, with a resolution of 12.5, is openly accessible through The Alaska Satellite Facility (ASF). CHIRPS data contribute to generating the rainfall map, while Sentinel-2 data is aid in land use land cover classification of the study area.

Initially, inventory data were collated from both Google Earth imagery and field surveys. The creation of a precise and reliable inventory map detailing soil erosion is deemed essential as the primary step towards developing a SESM for the study area (Aslam *et al.*, 2021). Both field investigations and Google Earth imagery were utilized to ensure the accuracy of the inventory map. Subsequently, two distinct datasets were generated from the inventory data: one designated for training purposes (80%) and the other for testing (20%). The predisposing parameters, including altitude, slope angle, aspect, curvature, lithology, land use land cover, road, rainfall data, and stream network, was derived from a combination of ground and satellite data utilizing GIS technology. Elevation, Slope, Aspect, curvature, drainage was calculated from dem data using specified spatial analysis tools. Sentinel-02 image was classified using supervised classification and the area was calculated at the end. The soil and lithology data was digitized from the

geological map of Pakistan. All the created variables were reclassified high weightage were given to the high influence in soil erosion factor and low weightage was given to the low influencing factor. The testing data and the training data were then compared in the excel sheet for getting the validation of the result by using overall accuracy formula. Subsequently, the interrelationship between causative factors and soil erosion inventory will be analyzed computationally. Finally, the SESM of the Kohat region is generated using the FR model and was validated using the AUCROC method.

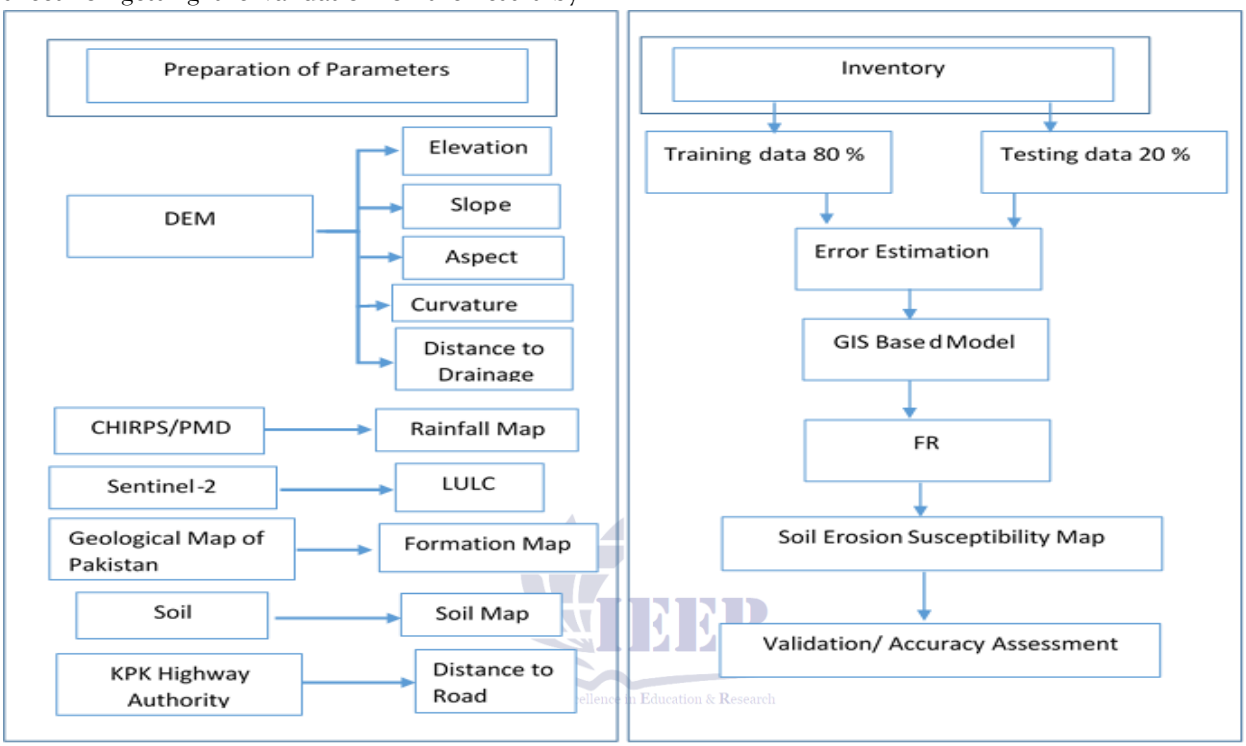

Figure 3.1 Comprehensive flowchart of the study

3.1 Frequency Ration Model (FRM)

The FR approach is one of the GIS-based algorithms that has received the most attention for assessing the spatial relationship between the two variables (Khosrokhani and Pradhan, 2014). This approach is a reliable tested technique for generating soil erosion map for the study region. This technique is a GIS based statistical approach that uses spatial data SESM (Bonham-Carter *et al.*, 1990; Chen et al., 2018; Senanayake *et al.*, 2020). The following Equation 1 was used for frequency ratio of soil erosion Susceptibility (Chen *et al.*, 2018).

$$FR = \frac{N_i S_x / M}{N_i l_s / Ml} \qquad (1)$$

Where FR = Frequency Ratio, $N_i S_x$ = number of pixels in each causative parameter category. M = total number of pixels, $N_i l_s$= soil erosion pixels number in parameter, Ml = total soil erosion pixels.

Then the following equation 2 were applied for SESP of FR.

$$SE = \sum_{i=1}^{n} FR_{ij} \qquad (2)$$

The above term FR_{ij} is the FR value for class 'j' of parameter 'i', n is the whole number of parameters.

Results and Discussion

4.1 Susceptibility maps

4.1.1 Elevation

Kohat's elevation has been taken out of the ALO and added to the DEM's corrected coordinate system to determine the area's elevation in meters, as seen in figure 4.1. The District Kohat's overall elevation ranges from 209 meters to 2061 meters. In east pf the study area the elevation is from 209 followed by the center of the study area and high elevation is in the west side of the Kohat District.

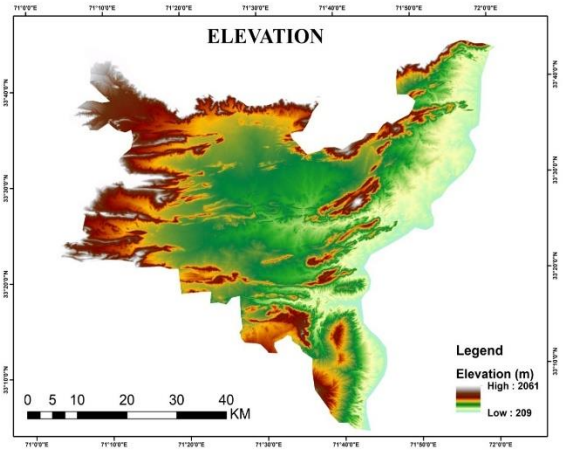

Figure 4.1 Map showing the elevation status

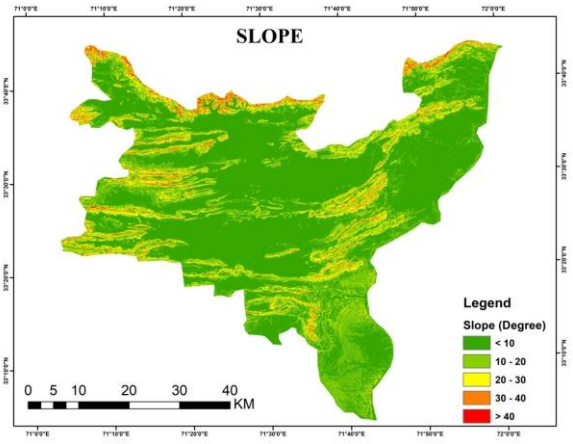

Figure 4.2 Map showing the Slope status

4.1.2 Slope

Using a slope analysis tool, the slope was extracted from the DEM. A key factor in soil erosion in the area is slope. Figure 4.2's result amply illustrates that the majority of the southern portion of the district has temperatures below 10 degrees. According to recent study, soil erosion occurs more frequently in temperatures between 10 and 20 and 30 degrees. 30 – 40 degree and above 40 degree was not to influencing in the soil erosion.

4.1.3 Aspect

Aspect variable is major effect on evapotranspiration and moisture content which lead to soil erosion the 09 figures that was carried out through Aspect Spatial analysis is given as under in figure 4.3. North side has 0-22.5, NE have 22.5-67.5, east 68.5-112.5, south 157.5-202.5. Most of the soil erosion factor in kohat is lies South area of the aspect most favorable to the soil erosion.

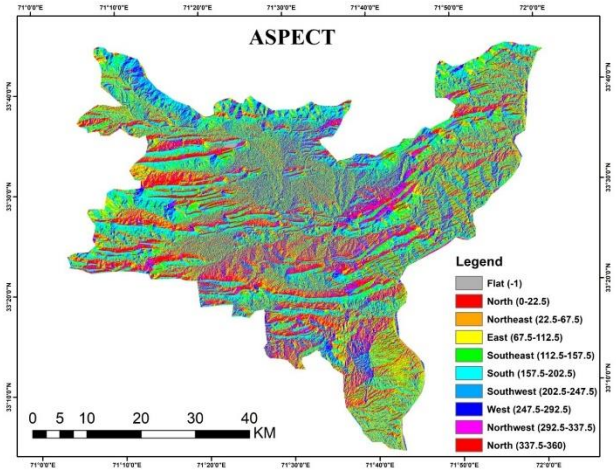

Figure 4.3 Map showing the Aspect Status

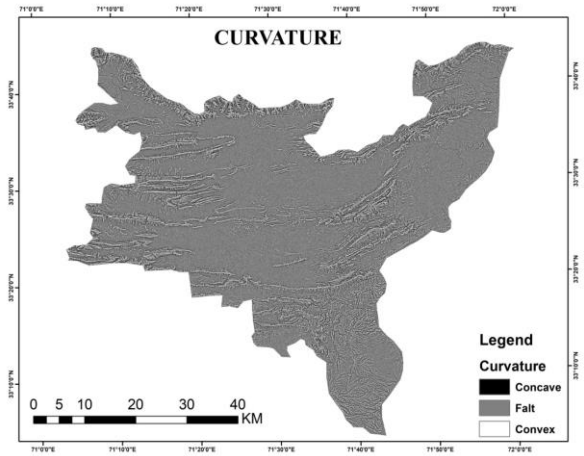

Figure 4.4 Map showing the Curvature status

4.1.4 Curvature

Useful information against geomorphology of the study area is through another spatial analysis of DEM data by Curvature tool, which Change the data of DEM to Concave, Flat and Convex Curvature. As shown in figure 4.4 the negative value in the study area from -14 to 0 was consider as concave, the 0 value which has no elevation are flat surface of the study area and the positive value from 1 to 18 is consider as convex.

4.1.5 Drainage

4.1.5.1 Hydrological Tools

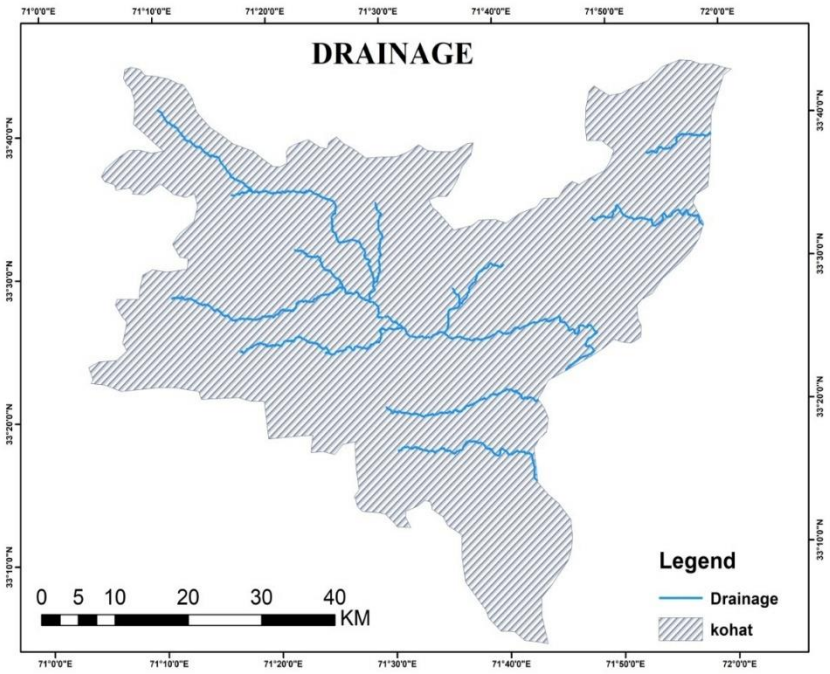

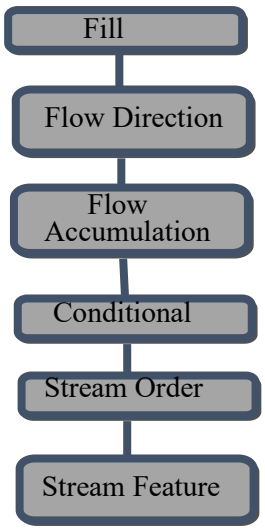

Figure 4.6 Map showing the Drainage status

4.1.5.2 Fill

The filling tool was pushed across the grid's surface to fill each well (DEM). Since they accounted for 0.9 to 4.7% of the total cell, these were depressions in a digital elevation model. Consequently, for these wells, the DEM backfill technique was employed. This tool creates the output area after the wells are filled, and it is received as a continuous grid area.

4. 1.5.3 Flow Direction

This tool allows you to determine the direction each grid cell flows in. In order to depict the direction of flow from each compartment toward its neighbor's steepest slope, the input and output grids are used by the tool to create a grid region (fill). "Force all cells to exit" is then chosen. Every cell in close proximity to the surface recedes from the grid's center.

4. 1.5.4 Flow Accumulation

Using this technique, the cumulative stream is calculated. A direction of flow grid is employed because the resultant grids display the cumulative run towards every cell. Each cell has the default weight of 1, as the input weight grid is optional. The data type of the output is integers. Once flows are accumulated to capture bigger flows, we split the gathered flow into two compartments.

4. 1.5.5 Conditional

When flow accumulation is set to true, the input true grid is utilized as the output cell value and the technique is functional to the grid surface in the way of flow. The database and the conditions output grid are lined up.

4.2 Euclidean Distance

The typical band area on a flat surface between binary subjects or lines is called the Euclidean distance. Each cell's distance from a source or group of sources is expressed in terms of Euclidean distance. To illustrate the figure's distance from the rest of the field, a visually appealing grid is created using a vector layer or another grid. Displays the available space at a given distance, another distance, etc. We've predefined the grid or there's a maximum distance specified. Each

4. 1.5.6 Focal Statistic

The focal statistics are computed by running the Focus Statistics program on the conditional grid. The conditional grid is seen in clear detail on the output centroid statistics grid. By default, the statistics type (optional), the district, and its settings are kept.

4. 1.5.7 Stream Order

In order to do this, workers in the flow system must be given a digital imperative. This technique aids in finding and categorizing generated flows according to the quantity of branches. The Flow Direction tool creates an input raster, and the Flow Order tool takes that raster and uses it to specify the flow direction of that raster. The flow direction is then used to determine the output raster. Flow networks that share the same flow order are categorized using the Spotlight technique. A primary and subsequent imperative connection do not form a third-directive connection; rather, they stay second-order connections.

4. 1.5.8 Stream to Feature

When vectorizing overlapping and neighboring cells, the Flow to Element tool is designed to make the best use of a directed grid. A linear flow network is represented by the flow grid surface that this tool uses as inputs. The flow direction tool is used to con ow direction raster, which contains the low in the flow base and is indicated as a shape file for the resultant polylines. The primary rivers in this study region are identified in response to this request.

section can be respectfully detached from its neighboring base thanks to the Euclidean distance manufacturing grid. In the grid projection unit, substitutions are identified and computed from one subject focus to the next.

4.3 Rainfall

Rainfall also is an important aspect to soil erosion. The data was prepared from CHIRPS data. The data was downloaded on yearly basis and in arc map we get the average rainfall data through raster

calculator.

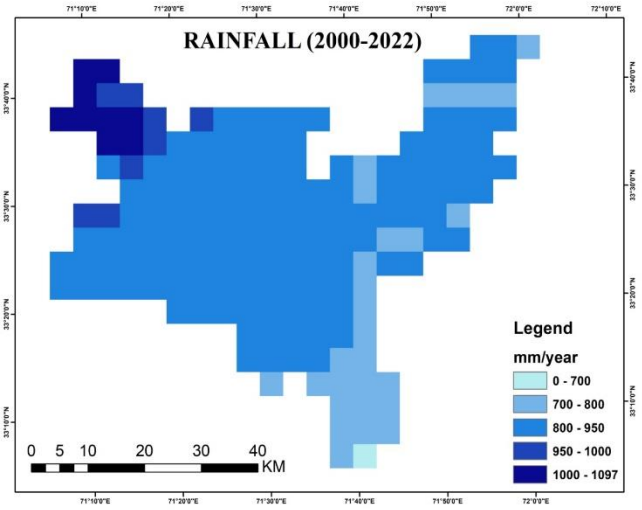

Figure 4.6 Map showing the Rainfall status

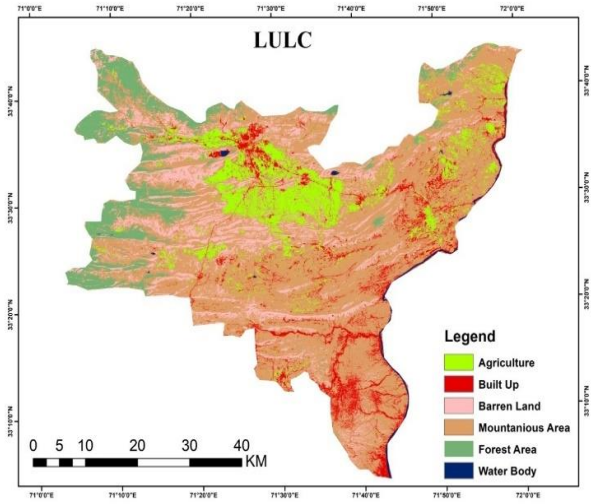

Figure 4.7 Map showing the LULC status

4.4 Image analysis Process

4.4 Image Classification

Land use land cover determined using Sentinel-02 images and then the classified result was validated with google earth using different Arc map tools.

4.4.1 Extraction

Using the Extract to mask tool, which extracts a grid cell that corresponds to the area, the extraction was completed. In order to extract the study area shape file, the grid from which the cell was retrieved is utilized as input. The form is allotted no data cells if the feature data is in raster format. Using sentinel-02 image, we utilized this application to extract our study region.

4.4.2 Supervised Classification

Afterwards, supervised classification by sampling is used to separate the Sentinel-2-extracted research area into several classes. The illustration originated from the menu bar's training example.

These training examples are then stored for use in noisy data categorization. To "create" a signature for these training examples, let's proceed. The route for classification is given by this signature. This tool accepts raster images as input, and it uses the image-created training example to input data into the feature example dataset. The location of the signature file output is chosen.

4.4.3 Maximum Likelihood Classification

Raster categorized layers are produced when ordinary raster strips are subjected to maximum likelihood classification. Both an input raster picture and an input signature file made with the Signature File tool are provided. In the output, select the categorized raster layer. Due to a portion of the cell not being classified during classification, the reject rate is kept by default in the tool. All of the raster layer's cells will be classified, nevertheless, if it is 0.0. All classes received the same priority because the prior probability option was selected equally.

4.5 lithology

The composition of lithology of the Kohat area was digitize from Pakistan Geological Survey data. The image was first rectified and the after that class wise data was digitized from the image. It consists of different formation like alluvium, metaphorphic, sedimentary etc. as shown in figure 4.7.

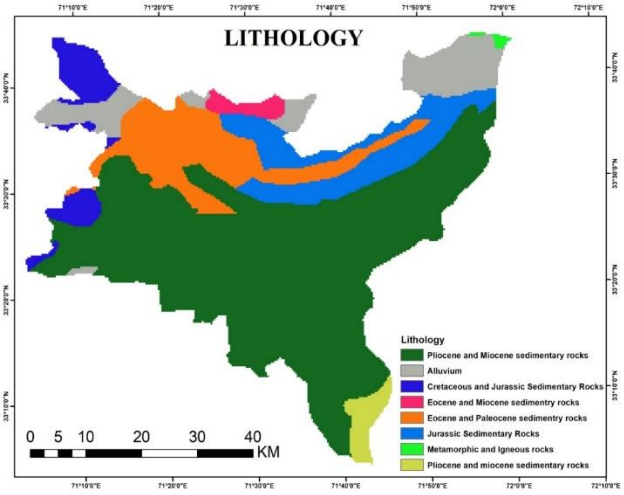

Figure 4.8 Map showing the Lithology status

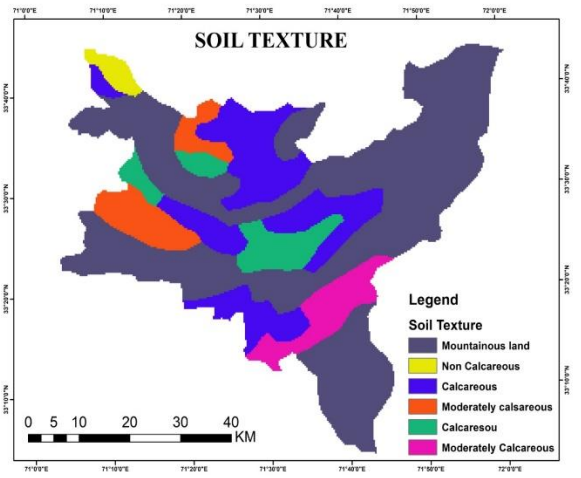

Figure 4.9 Map showing the Soil texture status

4.6 Soil Texture

Soil texture was digitized from the geological survey of Pakistan. Texture of the soil is essential aspect to soil erosion, it also impacts the structure of the soil, like mountainous land, non-calcareous, calcareous, moderately calcareous, Loam and calcareous.

4.7 Reclassifying Data Sets

All raster datasets were produced with different techniques. In order to create a prepared suitability map that would identify irrigated regions in the District Kohat, the derived grid surface layer was kept together. Now, each grid region has a new ranking and weight based on its relative relevance. The high percentage rate was for high erodibility area and the low percentage of the area was given as low erodibility area. The reclassification was done for all the layers to prepare the results for the weighted overlay.

4.8 Reclassify Elevation

The Elevation that was taken from ALOS was reclassified according to their importance. High value was given to the high eroded risk areas and low value was given to the low influence area. As shown in table 4.1.

Table 4.1: Table Showing Criteria for Elevation

Class Range	Weight	Description
< 400	5	High
400 - 600	3	Moderate
600 - 800	2	Low
>1000	1	Least

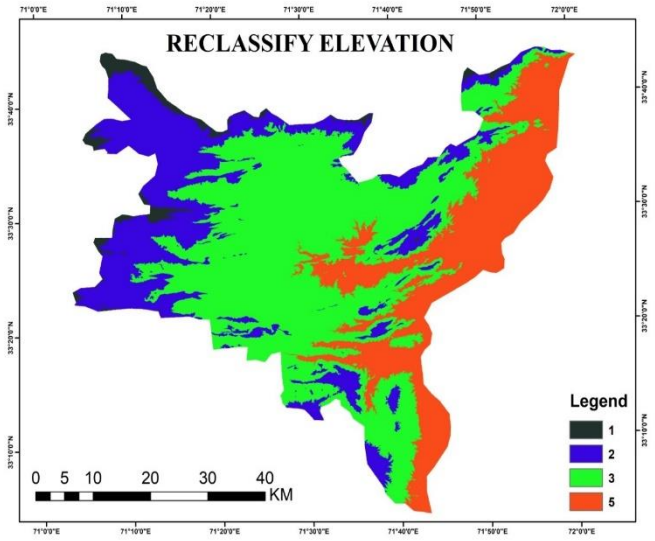

Figure 4.10 Map showing the Reclassify Elevation status

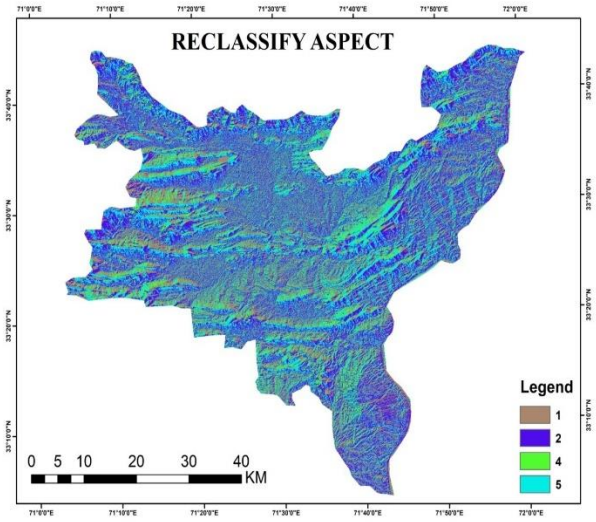

Figure 4.11Map showing the Reclassify Aspect status

4.9 Reclassify Aspect

The Aspect is reclassified, divided the value on the basis of SW was given high ranked and the remaining was followed by 4 and 2. Value of 5 is assigned to high and the value of 1 to the Low Ranked value area given below:

4.10 Reclassify Curvature

The output of the Curvature is reclassified, divided the value into Convex, flat and concave. The high Value of 5 is assigned to convex low value was assigned to the flat surface where there is no soil erosion can occurred and medium weights were given to concave high influence and the value of 1 to the low influence. As shown in table 4.2.

Table 4.2: Table Showing Criteria for Curvature

Class Range	Weight	Description
Concave	2	High
Flat	1	Moderately
Convex	5	Less

4.11 Reclassify Slope

Output of the slope were reclassified into 5 categories. Value 5 were assigned to high influence area and 1 to less influence area. The ranked value is given below:

Table 4.3: Table showing criteria for classified slope

Class range (feet)	Weight	Description
<10	3	Moderate
10-20	5	High
20-30	4	Moderately
30-40	2	Low
>40	1	Least

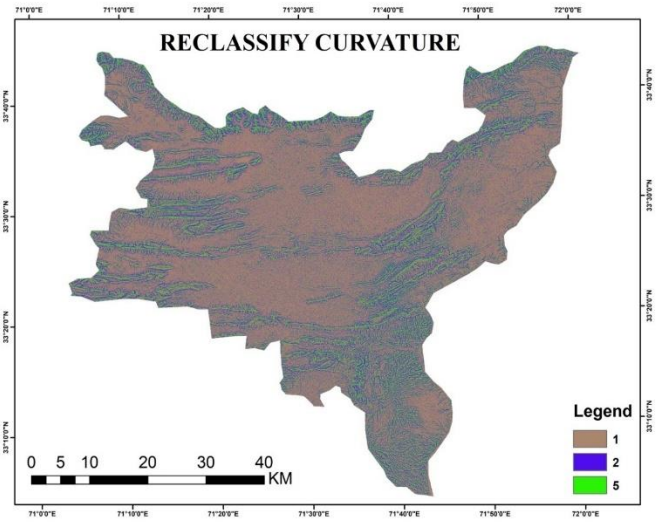

Figure 4.12 Map showing the Reclassify Curvature status

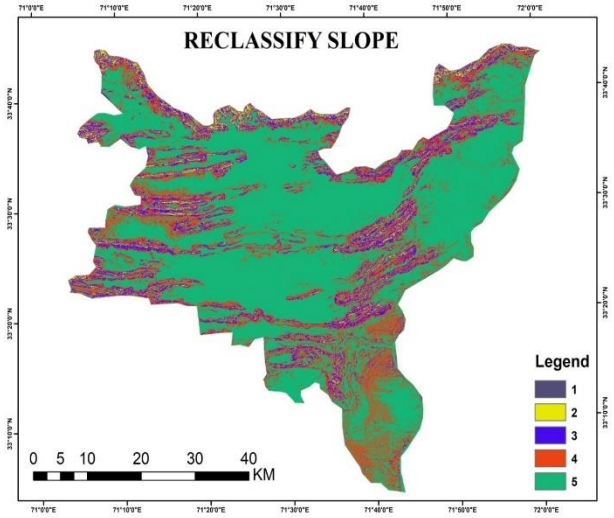

Figure 4.13 Map showing the Reclassify Slope status

4.12 Reclassify Rivers

The result of Euclidean distance was reclassified 5 value is given as high influence, 4 and 3 moderate and 1 value is given to far away the area of river above 350m which is less influence.

Table 4.4: Table showing criteria for reclassified river

Class Range	Weight	Description
<40	5	High
40-150	4	Moderately
150-250	3	Medium
250-350	2	Low
>350	1	Least

4.13 Reclassify Road

The resultant reclassifying the road's Euclidean distance, the value is divided into equal intervals. A 5 represents a high value, whereas a 1 represents a low value. Value area with rankings is shown below.

Table 4.5: Table Showing Criteria for Road

Class Range	Weight	Description
<25	4	High
25-50	3	Moderately
50-150	2	Medium
150-250	2	Low
>250	1	Least

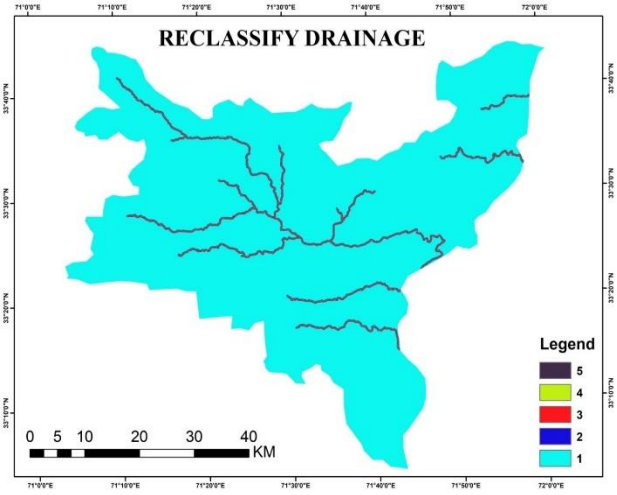

Figure 4.14 Map showing the Reclassify Drainage status

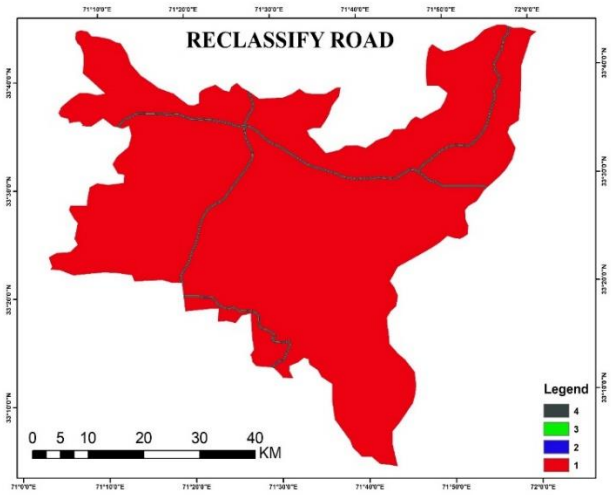

Figure 4.15 Map showing the Reclassify Roads status

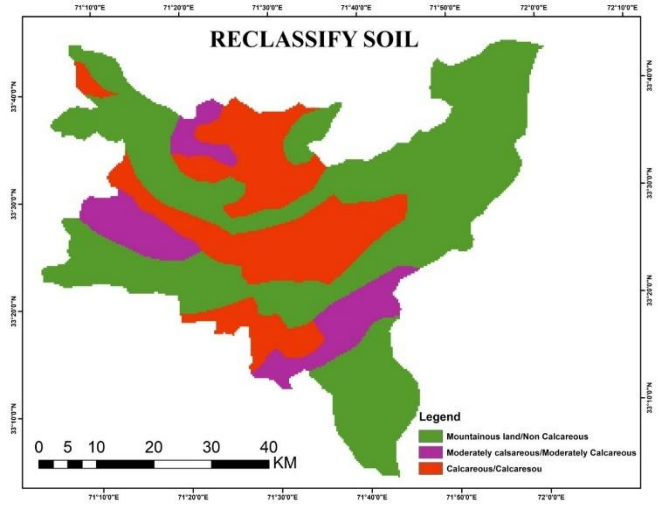

Figure 4.16 Map showing the Reclassify Soil texture status

4.14 Reclassify Soil Texture

Soil layer is first converted to raster before being reclassified. Mountainous, Moderately Calcareous, loam and clay. Loam and clay soils are highly valued, whereas mountainous are given a low rating. The value is ranked below:

Table 4.6: Table Showing Criteria for Classified Soil texture

Soil texture	Weight	Description
Loam & Clay (Calcareous)	5	High
Mountainous	4	Moderately
Moderately Calcareous	3	Less

4.15 Reclassify LULC

LULC was reclassified according to the classes as the other classes were mainly hitting the north area and center of the area for soil erosion however we can also take the satellite data and giving high value that have strong capability to erode the land.

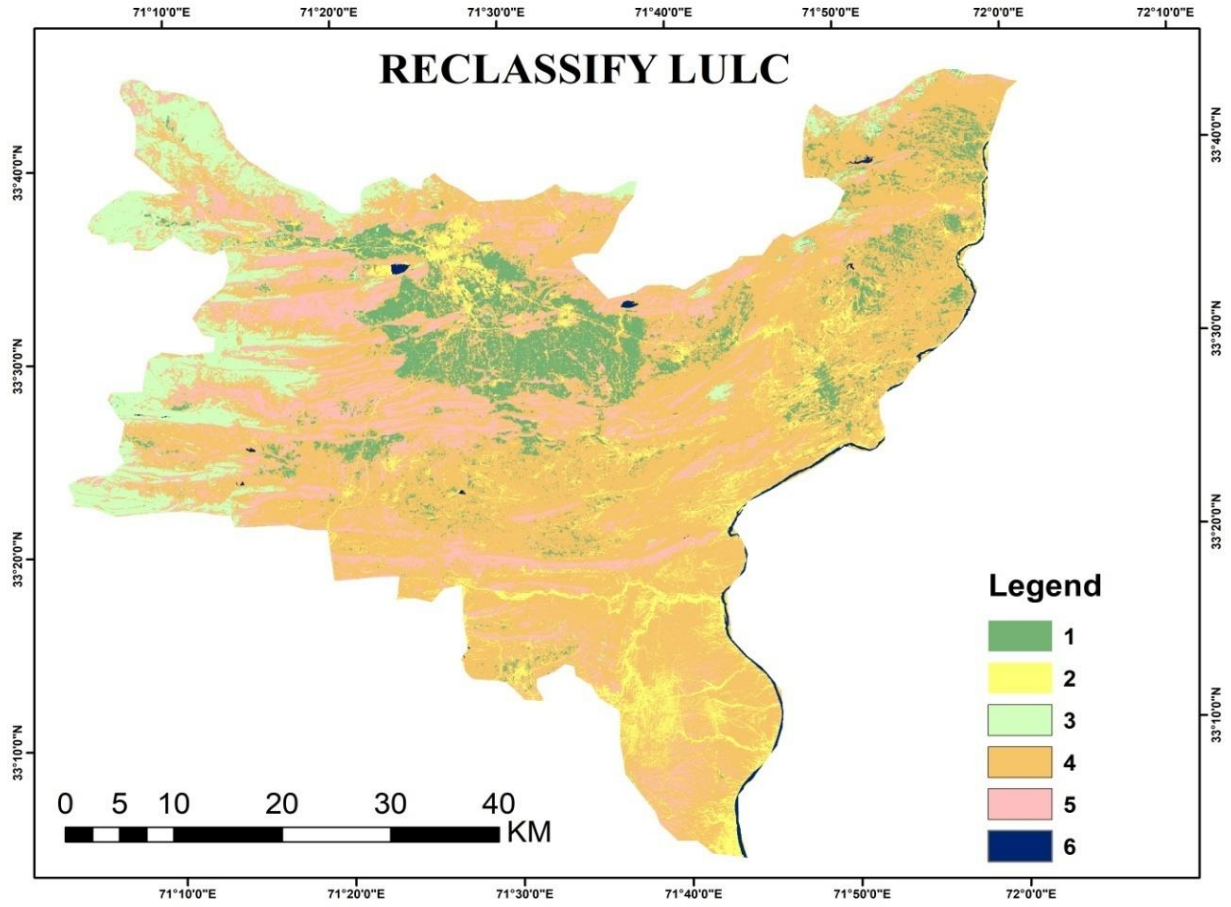

Figure 4.17 Map showing the Reclassify LULC status

4.16 Multi Influencing Factor

A final weighted overlay procedure combines all reclassified layers to create a single-layer map from each of the several parameter layers. The multi-influencer technique was used to weight each input grid according to its significance or degree of influence. This method is predicated on the primary and secondary impacts. The primary impact factors identified in our investigation were rivers and dams. While soil structure, slope and land use/cover received a smaller factor. Both the main impact (A) and the secondary effect (B) cumulative weights are used for determining relative rates. Each influencing factor's score is then determined using this rate. The formula is used to determine each influencing factor's suggested score.

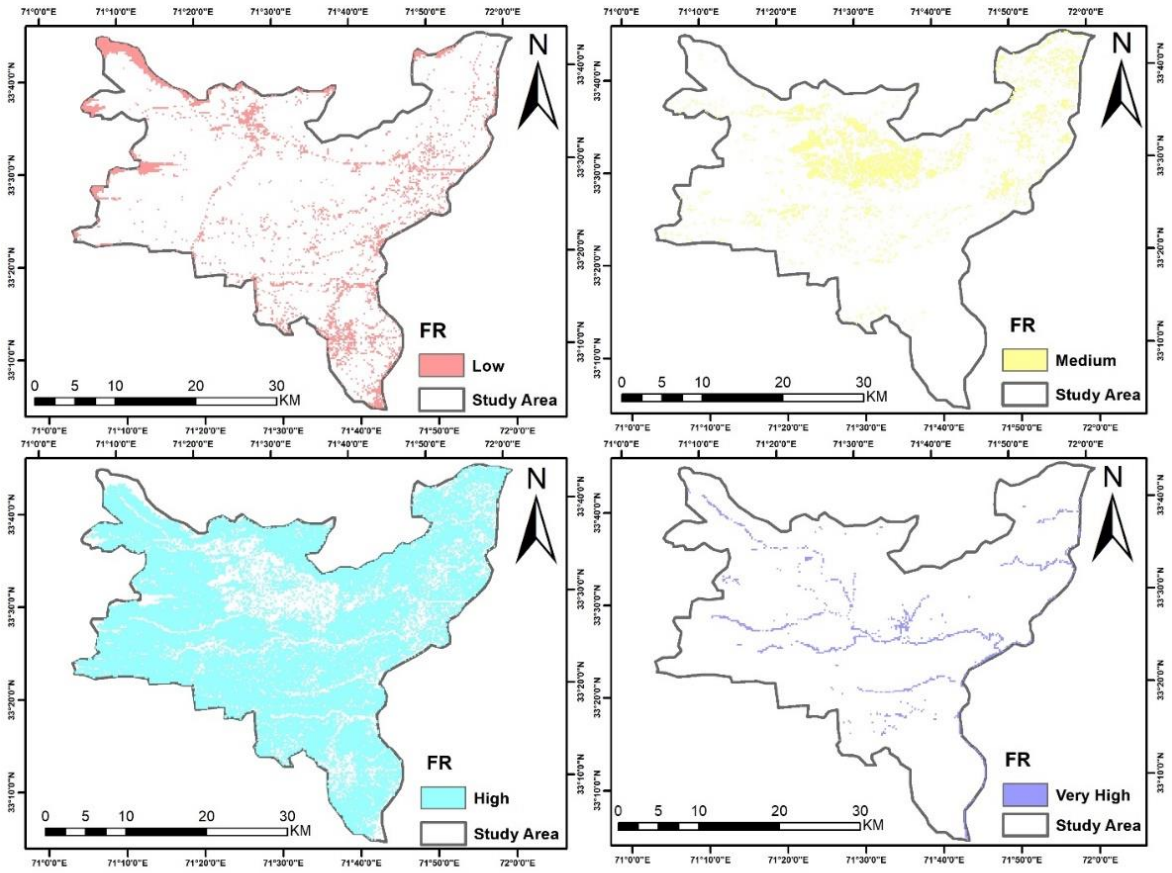

Figure 4.18 Maps showing the different susceptibility status

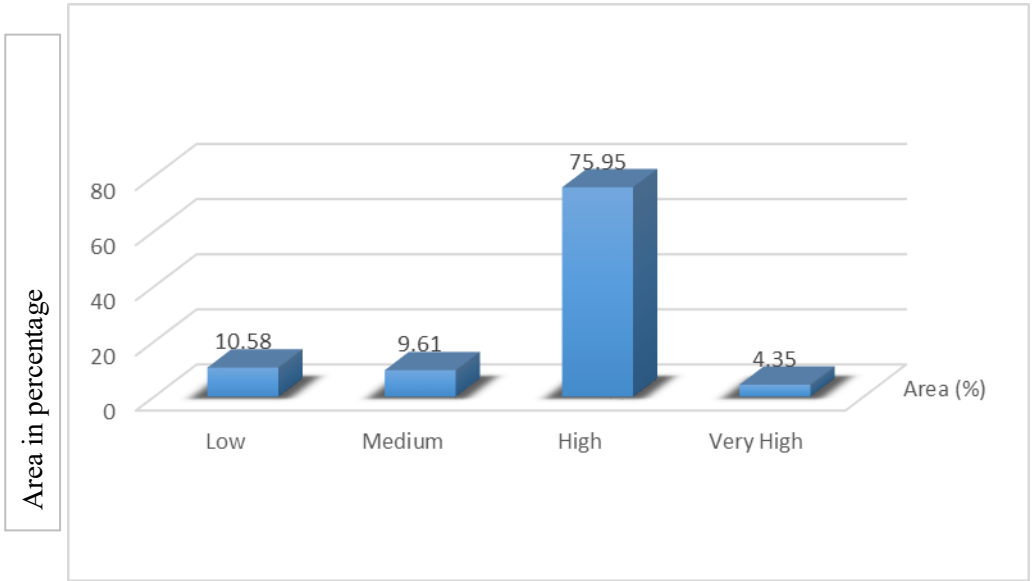

Figure 4.19 Graph showing the Percentage of the Susceptibility of District Kohat

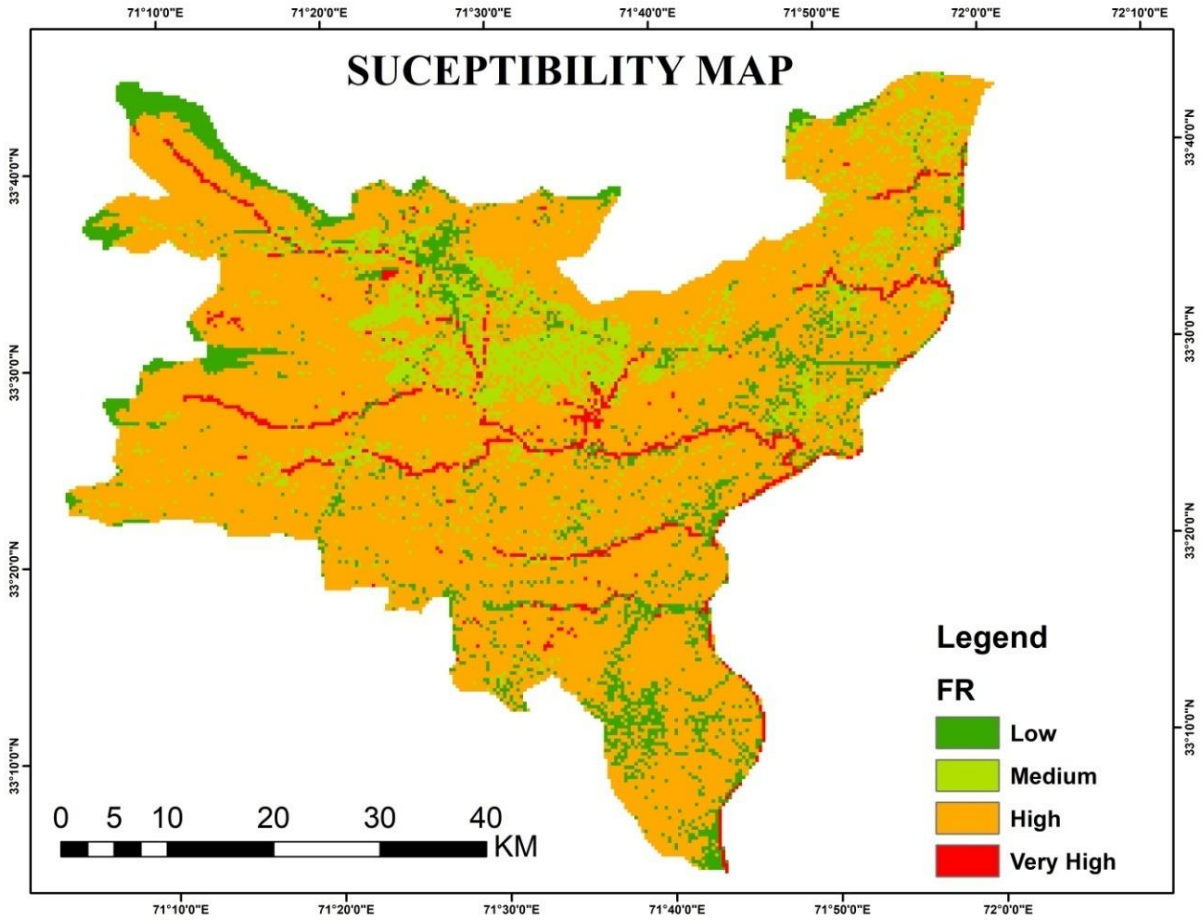

Figure 4.20 Map showing the Susceptibility status of District Kohat

The rate of land loss is higher than the rate of land development worldwide by a ratio of 10 to 40, endangering the environment and food security (the average annual rate of soil loss in Asia is 29.95 t/ha/year). This underscores the seriousness of the problem. Approximately 80% of the sediment discharged into the world's oceans is a result of soil conservation initiatives (Price et al., 2014; Naqvi et al., 2013). Degradation percentage of agricultural land worldwide (Puente et al., 2019) The effects are extensive and include decreased agricultural yield, changed water quality, a higher risk of landslides in steep terrain, sediment deposition in catchment water systems, which raises the possibility of flooding, and a decrease in the amount of energy produced from hydroelectric power (Alexander et al., 2012). Measurement of soil erosion, spatial mapping of its distribution, and vulnerability analysis-based area at risk identification are among the sustainable management techniques needed to address these difficulties (Koirala et al., 2019). For efficient mitigation and management, this research methodology for mapping soil erosion susceptibility is crucial. This project's goal is to create a reliable and precise soil erosion vulnerability mapping system that can locate and forecast locations within a given geographic area that are prone to erosion. This system will generate comprehensive vulnerability maps by utilizing machine learning algorithms, remote sensing techniques, and sophisticated geospatial data. MIF, which absorbed numerous conditions, was used to do this. Elevation, aspect, curvature, slope, drainage, roads, LULC, lithology, soil texture, and precipitation by superimposing weighted layers. The erratic places that contributed appropriately to soil erosion were given a lot of attention.

Rainfall is extremely susceptible to soil erosion, along with elevation, aspect, curvature, slope, and drainage. You can rapidly locate and contrast hot regions thanks to the suitability map that presents the data in (Figure 4.18). In summary, Kohat has a relatively high erosion rate (4% overall), with high, medium, and low sensitivity levels following shown in figure 4.19 and 20. This is especially evident along the river. Sustainable land management techniques, conservation programs, and land use planning will all be based on these maps. The produced maps enable erosion prevention and control strategies to be prioritized by giving decision makers access to relevant information. In the end, this project's vulnerability map will be a useful tool for sustainable development, land management, and conservation initiatives. This will provide stakeholders with the information they need to decide how best to promote sustainable land use practices and reduce soil erosion.

Conclusion

5.1 Conclusion

The outcome yielded a map that classified the Kohat district's irrigated land suitability into four categories: low, medium, high, and extremely high. The results of the study will be useful in the formulation of plans and policies by the Pakistani government and other non-governmental organizations to address soil erosion in the Kohat district.

A susceptibility map of eroded sites was created in this study using a GIS based multi-criteria analysis. Several technologies for spatial analysis were used to support this. Five layers were used to apply the tool: LULC, Path, Drainage, Aspect, Curvature, Slope, and Precipitation.

The outcomes of this investigation demonstrate how the geographic information system may be employed as a tool to methodically examine water resources, resulting in a more accurate and serene analysis. The adoption of an unparalleled worldwide approach may be one of the study's main takeaways for investors, management, and other stakeholders.

References

Agarwal, D., Tongaria, K., Pathak, S., Ohri, A., &Jha, M. (2016). Soil erosion mapping of watershed in Mirzapur district using RUSLE model in GIS environment. *IJSRTM*, *4*(3), 56-63.

Aggarwal, C.C., 2020. Neural networks and deep learning. SpringerCC AggarwalSpringer,.

Akgün, A., Türk, N., 2011. Mapping erosion susceptibility by a multivariate statistical method: A case study from the Ayvalik region, NW Turkey. Comput. Geosci. 37, 1515–1524. https://doi.org/10.1016/j.cageo.2010.09.006.

Alexander, J.L., Mohd Sidek, L., Mohamed Desa, M.N., Julien, P.Y., 2012. Challenge in Running Hydropower As Source of Clean Energy : Ringlet Reservoir , Cameron Highlands Case Study. Proc. Natl. Grad. Conf. 2012 2012, 8–10.

Arabameri, A., Chen, W., Loche, M., Zhao, X., ... Y.L.-G., undefined 2020, 2022. Comparison of machine learning models for gully erosion susceptibility mapping. Elsevier.

Arabameri, A., Pal, S.C., Costache, R., Saha, A., Rezaie, F., Danesh, A.S., Pradhan, B., Lee, S., Hoang, N.-D., 2021. Prediction of gully erosion susceptibility mapping using novel ensemble machine learning algorithms. Taylor Fr. Arab. S Chandra Pal, R Costache, A Saha, F Rezaie, A Seyed Danesh, B PradhanGeomatics, Nat. Hazards Risk, 2021•Taylor Fr. 12, 469–498. https://doi.org/10.1080/19475705.2021.1880977.

Aslam, B., Maqsoom, A., Salah Alaloul, W., Ali Musarat, M., Jabbar, T., Zafar, A., 2021. Soil erosion susceptibility mapping using a GIS-based multi-criteria decision approach: Case of district Chitral, Pakistan. Ain Shams Eng. J. 12, 1637–1649. https://doi.org/10.1016/j.asej.2020.09.015.

Azra, A., Kaleemullah, M., Khattak, B., Asma, N., Safi, A.U.R., Qaiser, J., Afzal, M., Tahir, U., Sindhu, Z.U.D., Farhan, Y., 2019. Comparative efficacy of domestic garlic (Allium Sativum) and neem (Azadirachta Indica) against Haemonchus Contortus in small ruminants. Appl. Ecol. Environ. Res. 17, 10389–10397. https://doi.org/10.15666/aeer/1705_1038910397.

Bonham-Carter, G.F., Agterberg, F.P., Wright, D.F., 1990. Integration of geological datasets for gold exploration in Nova Scotia. Introd. readings Geogr. Inf. Syst. 10, 170–182. https://doi.org/10.1029/sc010p0015.

Biswas, H., Raizada, A., Mandal, D., Kumar, S., Srinivas, S., & Mishra, P. K. (2015). Identification of areas vulnerable to soil erosion risk in India using GIS methods. *Solid Earth*, 6(4), 1247-1257.

Chakrabortty, R., Pal, S.C., Chowdhuri, I., Malik, S., Das, B., 2020. Assessing the Importance of Static and Dynamic Causative Factors on Erosion Potentiality Using SWAT, EBF with Uncertainty and Plausibility, Logistic Regression and Novel Ensemble Model in a Sub-tropical Environment. J. Indian Soc. Remote Sens. 2020 485 48, 765–789. https://doi.org/10.1007/S12524-020-01110-X.

Chen, W., Li, H., Hou, E., Wang, S., Wang, G., Panahi, M., Li, T., Peng, T., Guo, C., Niu, C., Xiao, L., Wang, J., Xie, X., Ahmad, B. Bin, 2018. GIS-based groundwater potential analysis using novel ensemble weights-of-evidence with logistic regression and functional tree models. Sci. Total Environ. 634, 853–867. https://doi.org/10.1016/J.SCITOTENV.2018.04.055.

Chen, W., Panahi, M., Catena, H.R.P.-, 2017. Performance evaluation of GIS-based new ensemble data mining techniques of adaptive neuro-fuzzy inference system (ANFIS) with genetic algorithm (GA). Elsevier.

Conoscenti, C., Agnesi, V., Angileri, S., Cappadonia, C., Rotigliano, E., Märker, M., 2013. A GIS-based approach for gully erosion susceptibility modelling: A test in Sicily, Italy. Environ. Earth Sci. 70, 1179–1195. https://doi.org/10.1007/S12665-012-2205-Y.

Conoscenti, C., Agnesi, V., Cama, M., Caraballo-Arias, N.A., Rotigliano, E., 2018. Assessment of Gully Erosion Susceptibility Using Multivariate Adaptive Regression Splines and Accounting for Terrain Connectivity. L. Degrad. Dev. 29, 724–736. https://doi.org/10.1002/LDR.2772.

Dinh, T Vu, Hoang, N.D., Applied, X.L.T.-, Soil, E., 2021. Evaluation of different machine learning models for predicting soil erosion in tropical sloping lands of Northeast Vietnam. hindawi.comT Vu Dinh, ND Hoang, XL TranApplied Environ. Soil Sci. 2021 • hindawi.com.

Dinh, Tuan Vu, Nguyen, H., Tran, X.L., Hoang, N.D., 2021. Predicting Rainfall-Induced Soil Erosion Based on a Hybridization of Adaptive Differential Evolution and Support Vector Machine Classification. Math. Probl. Eng. 2021. https://doi.org/10.1155/2021/6647829.

El-Magd, S.A.A., Ali, S.A., Pham, Q.B., 2021. Spatial modeling and susceptibility zonation of landslides using random forest, naïve bayes and K-nearest neighbor in a complicated terrain. Earth Sci. Informatics 14, 1227–1243. https://doi.org/10.1007/S12145-021-00653-Y.

Ettazarini, S., Jakani, M. El, Najoui, K., 2017. Assessment of Soil Loss Risk Using Integrated Remote Sensing and Geographic Information System (GIS) Techniques in the Argana Basin, Morocco. Am. J. Innov. Res. Appl. Sci. 320, 186–194.

Ganasri, B.P., Ramesh, H., 2016. Assessment of soil erosion by RUSLE model using remote sensing and GIS - A case study of Nethravathi Basin. Geosci. Front. 7, 953–961.https://doi.org/10.1016/j.gsf.2015.10.007.

Gayen, A., Pourghasemi, H.R., Saha, S., of the total ..., S.K.-S., 2020. Gully erosion susceptibility assessment and management of hazard-prone areas in India using different machine learning algorithms. Elsevier.

Gayen, A., Saha, S., 2017. Application of weights-of-evidence (WoE) and evidential belief function (EBF) models for the delineation of soil erosion vulnerable zones: a study on Pathro river basin, Jharkhand, India. Model. Earth Syst. Environ. 3, 1123–1139. https://doi.org/10.1007/S40808-017-0362-4.

Gayen, A., Saha, S., Pourghasemi, H.R., 2019a. Soil erosion assessment using RUSLE model and its validation by FR probability model. Geocarto Int. https://doi.org/10.1080/10106049.2019.1581272.

Gayen, A., Saha, S., Pourghasemi, H.R., 2019b. Soil erosion assessment using RUSLE model and its validation by FR probability model. Geocarto Int. 0, 000. https://doi.org/10.1080/10106049.2019.1581272.

Gholami, V., Sahour, H., Catena, M.A.H.A.-, 2021. Soil erosion modeling using erosion pins and artificial neural networks. Elsevier.

Gong, W., Liu, T., Duan, X., Sun, Y., Zhang, Y., Tong, X., Qiu, Z., 2022. Estimating the Soil Erosion Response to Land-Use Land-Cover Change Using GIS-Based RUSLE and Remote Sensing: A Case Study of Miyun Reservoir, North China. Water 2022, Vol. 14, Page 742 14, 742. https://doi.org/10.3390/W14050742.

Haregeweyn, N., Tsunekawa, A., of the Total ..., J.P.-S., 2017. Comprehensive assessment of soil erosion risk for better land use planning in river basins: Case study of the Upper Blue Nile River. Elsevier.

Hembram, T.K., Paul, G.C., Saha, S., 2019. Comparative Analysis between Morphometry and Geo-Environmental Factor Based Soil Erosion Risk Assessment Using Weight of Evidence Model: a Study on Jainti River Basin, Eastern India. Environ. Process. 6, 883–913. https://doi.org/10.1007/S40710-019-00388-5/FIGURES/13.

Hussain, M.A., 2014. Seroprevalence of Brucellosis in Sheep and Humans in District Kohat, Pakistan. Adv. Anim. Vet. Sci. 2, 516–523. https://doi.org/10.14737/journal.aavs/2014/2.9.516.523.

Hussain, S.A., Han, F.Q., Ma, Z., Hussain, A., Mughal, M.S., Han, J., Alhassan, A., Widory, D., 2021. Origin and Evolution of Eocene Rock Salts in Pakistan and Implications for Paleoclimate Studies: Insights From Chemistry and Cl Stable Isotopes. Front. Earth Sci. 9. https://doi.org/10.3389/FEART.2021.644485/FULL.

Igwe, O., John, U.I., Solomon, O., Obinna, O., 2020. GIS-based gully erosion susceptibility modeling, adapting bivariate statistical method and AHP approach in Gombe town and environs Northeast Nigeria. Geoenvironmental Disasters 7. https://doi.org/10.1186/s40677-02-00166-8.

Jabbar, F.K., Grote, K., Tucker, R.E., 2019. A novel approach for assessing watershed susceptibility using weighted overlay and analytical hierarchy process (AHP) methodology: a case study in Eagle Creek Watershed, USA. Environ. Sci. Pollut. Res. 26, 31981–31997. https://doi.org/10.1007/s11356-019-06355-9.

Jebur, M.N., Pradhan, B., of Environment, M.S.T.-R.S., undefined 2014, 2014. Optimization of landslide conditioning factors using very high-resolution airborne laser scanning (LiDAR) data at catchment scale.Elsevier.https://doi.org/10.1016/j.rse.2014.05.013.

Jha, M.K., of Spatial Hydrology, R.C.P.-J., undefined 2010, n.d. Erosion Predictions by Empirical Models in a Mountainous Watershed in Nepal. search.ebscohost.comMK Jha, RC PaudelJournal Spat. Hydrol.

2010 • search.ebscohost.com.

Krishna Bahadur, K. C. (2009). Mapping soil erosion susceptibility using remote sensing and GIS: a case of the Upper Nam WA Watershed, Nan Province, Thailand. *Environmental geology*, *57*, 695-705.

Kashiwar, S.R., Kundu, M.C., Dongarwar, U.R., 2022. Soil erosion estimation of Bhandara region of Maharashtra, India, by integrated use of RUSLE, remote sensing, and GIS. Nat. Hazards 110, 937–959. https://doi.org/10.1007/S11069-021-04974-5.

Kavzoglu, T., Colkesen, I., Sahin, E.K., 2019. Machine learning techniques in landslide susceptibility mapping: A survey and a case study. Adv. Nat. Technol. Hazards Res. 50, 283–301. https://doi.org/10.1007/978-3-319-77377-3_13.

Khosrokhani, M., Pradhan, B., 2014. Spatio-temporal assessment of soil erosion at Kuala Lumpur metropolitan city using remote sensing data and GIS. Geomatics, Nat. Hazards Risk 5, 252–270. https://doi.org/10.1080/19475705.2013.794164.

Koirala, P., Thakuri, S., Joshi, S., Chauhan, R., 2019. Estimation of Soil Erosion in Nepal using a RUSLE modeling and geospatial tool. Geosci. 9. https://doi.org/10.3390/geosciences9040147.

Lu, D., Li, G., Valladares, G. S., &Batistella, M. (2004). Mapping soil erosion risk in Rondonia, Brazilian Amazonia: using RUSLE, remote sensing and GIS. *Land degradation & development*, *15*(5), 499-512.

Liu, M., Han, G., 2020. Assessing soil degradation under land-use change: Insight from soil erosion and soil aggregate stability in a small karst catchment in southwest China. PeerJ 2020. https://doi.org/10.7717/peerj.8908.

Madarász, B., Jakab, G., Szalai, Z., Soil, K.J.-, ... T., 2021. Long-term effects of conservation tillage on soil erosion in Central Europe: A random forest-based approach. Elsevier.

Maity, D.K., Mandal, S., 2019. Identification of groundwater potential zones of the Kumari river basin, India: an RS & GIS based semi-quantitative approach. Environ. Dev. Sustain. 21, 1013–1034. https://doi.org/10.1007/S10668-017-0072-0.

Mararakanye, N., Geomorphology, P.D.S.-, 2017. Gully erosion: A comparison of contributing factors in two catchments in South Africa. Elsevier.

Meena, S.R., Ghorbanzadeh, O., international journal of, T.B.-I., undefined 2019, 2023. A comparative study of statistics-based landslide susceptibility models: A case study of the region affected by the gorkha earthquake in nepal. mdpi.comSR Meena, O Ghorbanzadeh, T BlaschkeISPRS Int. J. geo-information, 2019 • mdpi.com.

Meshram, S.G., Singh, V.P., Kisi, O., Karimi, V., Meshram, C., 2020. Application of Artificial Neural Networks, Support Vector Machine and Multiple Model-ANN to Sediment Yield Prediction. Water Resour. Manag. 34, 4561–4575. https://doi.org/10.1007/S11269-020-02672-8.

Mosavi, A., Sajedi-Hosseini, F., Choubin, B., Taromideh, F., Rahi, G., Dineva, A.A., 2020. Susceptibility mapping of soil water erosion using machine learning models. Water (Switzerland) 12, 1–17. https://doi.org/10.3390/w12071995.

Naqvi, H.R., Mallick, J., Devi, L.M., Siddiqui, M.A., 2013. Multi-temporal annual soil loss risk mapping employing Revised Universal Soil Loss Equation (RUSLE) model in Nun Nadi Watershed, Uttrakhand (India). Arab. J. Geosci. 6, 4045–4056. https://doi.org/10.1007/S12517-012-0661-Z.

Nekhay, O., Arriaza, M., of environmental management, L.B.-J., undefined 2009, 2009. Evaluation of soil erosion risk using Analytic Network Process and GIS: A case study from Spanish mountain olive plantations. Elsevier 90, 3091–3104. https://doi.org/10.1016/j.jenvman.2009.0

4.022.

Paul, S.S., Li, J., Li, Y., Shen, L., 2021. Assessing land use–land cover change and soil erosion potential using a combined approach through remote sensing, RUSLE and random forest algorithm. Geocarto Int. 36, 361–375. https://doi.org/10.1080/10106049.2019.1614099.

Persichillo, M.G., Bordoni, M., of the total environment, C.M.-S., undefined 2017, 2017. The role of land use changes in the distribution of shallow landslides. Elsevier.

Pourghasemi, H.R., Pradhan, B., Gokceoglu, C., 2012. Application of fuzzy logic and analytical hierarchy process (AHP) to landslide susceptibility mapping at Haraz watershed, Iran. Nat. Hazards 63, 965–996. https://doi.org/10.1007/S11069-012-0217-2.

Prasannakumar, V., Shiny, R., Geetha, N., Vijith, H., 2011. Spatial prediction of soil erosion risk by remote sensing, GIS and RUSLE approach: A case study of Siruvani river watershed in Attapady valley, Kerala, India. Environ. Earth Sci. 64, 965–972. https://doi.org/10.1007/S12665-011-0913-3.

Price, G., Alam, R., Hasan, S., Humayun, F., Kabir, M.H., 2014. Attitudes to water in South Asia.

Puente, C., Olague, G., Trabucchi, M., Arjona-Villicaña, P.D., Soubervielle-Montalvo, C., 2019. Synthesis of Vegetation Indices using genetic programming for soil erosion estimation. Remote Sens. 11, 1–25. https://doi.org/10.3390/rs11020156.

Rahmati, O., Tahmasebipour, N., Geomorphology, A.H.-, 2017. Evaluation of different machine learning models for predicting and mapping the susceptibility of gully erosion. Elsevier.

Saha, S., Gayen, A., Pourghasemi, H.R., Tiefenbacher, J.P., 2019. Identification of soil erosion-susceptible areas using fuzzy logic and analytical hierarchy process modeling in an agricultural watershed of Burdwan district, India. Environ. Earth Sci. 78. https://doi.org/10.1007/s12665-019-8658-5.

Saha, S., Roy, J., Arabameri, A., Blaschke, T., Sensors, D.T.B.-, undefined 2020, 2020.Machine learning-based gully erosion susceptibility mapping: A case study of Eastern India. mdpi.comS Saha, J Roy, A Arab. T Blaschke, D Tien BuiSensors.

Sepuru, T. K., &Dube, T. (2018). An appraisal on the progress of remote sensing applications in soil erosion mapping and monitoring. *Remote Sensing Applications: Society and Environment*, *9*, 1-9.

Sahaar, A.S., Julien, P.Y., Arabi, M., Kampf, S.K., 2013. Erosion mapping and sediment yield of the Kabul River Basin, Afghanistan.

Senanayake, S., Pradhan, B., Huete, A., Brennan, J., 2020. Assessing soil erosion hazards using land-use change and landslide frequency ratio method: A case study of Sabaragamuwa province, Sri Lanka. Remote Sens. 12. https://doi.org/10.3390/RS12091483

Sharma, N.K., Singh, R.J., Mandal, D., Agriculture, A.K.-, undefined ecosystems, undefined 2017, 2019. Increasing farmer's income and reducing soil erosion using intercropping in rainfed maize-wheat rotation of Himalaya, India. Elsevier.

Smith, P., House, J.I., Bustamante, M., Sobocká, J., Harper, R., Pan, G., West, P.C., Clark, J.M., Adhya, T., Rumpel, C., Paustian, K., Kuikman, P., Cotrufo, M.F., Elliott, J.A., Mcdowell, R., Griffiths, R.I., Asakawa, S., Bondeau, A., Jain, A.K., Meersmans, J., Pugh, T.A.M., 2016. Global change pressures on soils from land use and management. Glob. Chang. Biol. 22, 1008–1028. https://doi.org/10.1111/gcb.13068.

Tang, Q., Xu, Y., Bennett, S.J., Li, Y., 2015. Assessment of soil erosion using RUSLE and GIS: a case study of the Yangou watershed in the Loess Plateau, China. Environ. Earth Sci. 73, 1715–1724. https://doi.org/10.1007/S12665-014-3523-Z.

Tehrany, M.S., Shabani, F., Javier, D.N., Kumar, L., 2017. Soil erosion susceptibility mapping for current and 2100 climate conditions using evidential belief function and frequency ratio. Geomatics, Nat. Hazards Risk 8, 1695–1714. https://doi.org/10.1080/19475705.2017.1384406.

Thapa, P., 2020. Spatial estimation of soil erosion using RUSLE modeling: a case study of Dolakha district, Nepal. Environ. Syst. Res. 9. https://doi.org/10.1186/S40068-020-00177-2

Vu, D.T., Tran, X.L., Cao, M.T., Tran, T.C., Hoang, N.D., 2020. Machine learning based soil erosion susceptibility prediction using social spider algorithm optimized multivariate adaptive regression spline. Measurement 164, 108066. https://doi.org/10.1016/J.MEASUREMENT.2020.108066.

Vu Dinh, T., Hoang, N.D., Tran, X.L., 2021. Evaluation of Different Machine Learning Models for Predicting Soil Erosion in Tropical Sloping Lands of Northeast Vietnam. Appl. Environ. Soil Sci. 2021. https://doi.org/10.1155/2021/6665485.

Yusof, M.F., Azamathulla, H.M., Abdullah, R., 2014. Prediction of soil erodibility factor for Peninsular Malaysia soil series using ANN. Neural Comput. Appl. 24, 383–389. https://doi.org/10.1007/s00521-012-1236-3.